

A Methodological Investigation of Physics-Informed Neural Networks for Multi-Mechanism Coupled Damage Effectiveness Prediction

**Yalong Wang, Xianming Shi*, Mifen Yang, Penghua Liu,
Cenyu Hu and Chao Chang**

Army Engineering University of the PLA Shijiazhuang Campus
Hebei 050003, China

Corresponding author: Xianming Shi (email: sxm@nudt.edu.cn)

This article is distributed under the Creative Commons by-nc-nd Attribution License.
Copyright © 2025 Hikari Ltd.

Abstract

Damage effectiveness prediction is a pivotal issue in weapon system design and operational application. However, the coupled multi-physics effects in complex environments and the scarcity of experimental data pose significant challenges to traditional predictive methodologies. To address these limitations, this paper proposes a damage effectiveness prediction method based on Physics-Informed Neural Networks (PINN). This approach integrates key physical mechanisms, including kinetic energy penetration, blast shockwave propagation, fragment lethality, and ricochet effects, and quantifies them as residual loss functions under mathematical constraints to construct a deep learning framework that incorporates prior physical knowledge. Experimental results demonstrate that the proposed model achieves a 63.3% reduction in Root Mean Square Error (RMSE) and a 42.3% decrease in Mean Absolute Error (MAE) on the test set. Furthermore, under conditions of 30%-70% training data, the model exhibits superior generalization capabilities compared to traditional Multilayer Perceptron (MLP) models. Physics-consistency validation confirms that the prediction results strictly adhere to the law of conservation of energy. Nevertheless, the model's capability to capture abrupt changes in physical parameters requires further enhancement, indicating a direction for future research. This study provides a novel, high-precision, and highly inter-

pretable technological pathway for damage effectiveness prediction, possessing both theoretical innovation and engineering application value.

Keywords: Damage Effectiveness Prediction; Physics-Informed Neural Networks (PINN); Multi-Mechanism Coupling; Data Sparsity; Deep Learning; Munition Design

1. Introduction

The prediction of damage effectiveness is a central issue in the design and operational application of weapon systems. Accurate damage prediction not only optimizes ammunition consumption, thereby enhancing operational cost-effectiveness, but also enables targeted improvements in munition design based on specific target characteristics, augmenting destructive power. However, in complex battlefield environments, the damage mechanisms of different munitions against diverse targets exhibit significant disparities, involving multi-physics coupling processes such as kinetic energy penetration, blast shockwave loading, fragment lethality, and ricochet effects. These damage mechanisms are intricately intertwined, forming a highly complex nonlinear system [1-4], which poses considerable challenges to the accurate prediction of damage effectiveness. Furthermore, authentic damage experiments are prohibitively expensive and entail substantial risks. The stringency of experimental conditions and the irreproducibility of the experimental process further lead to a severe sparsity of available data, thereby constraining the precision and reliability of predictive models.

Currently, data-driven methodologies are extensively employed in the domain of damage effectiveness prediction, with neural networks and deep learning techniques emerging as prominent research foci. Scholars have endeavoured to introduce these advanced technologies into damage effectiveness prediction. For instance, Xue et al. [5] introduced an Intuitionistic Fuzzy Neural Network (IFNN) to predict parameters within the fragment damage field, leveraging the robust feature extraction capabilities of IFNN to capture the spatial characteristics of fragment distribution, thereby achieving a certain degree of predictive accuracy. Hou et al. [6] proposed an adaptive fuze-warhead coordination method based on a Backpropagation Artificial Neural Network (BP-ANN), which effectively predicts damage effectiveness at different radial positions by determining the optimal detonation location. Wang et al. [7] considered the factors influencing the pressure distribution patterns of dynamic explosion shockwaves and constructed predictive models for static and dynamic explosion shockwave pressures based on BP neural networks. Recognizing the nonlinearity and complexity inherent in target damage assessment, Xu et al. [8] utilized deep learning to develop a neural network imbued with expert experience for predicting radar target damage effects. Zhou et al. [9] employed an acoustic-structure algorithm to simulate the non-contact underwater explosion of a stiffened cylindrical shell section and established a damage effectiveness prediction model based on a machine learning backpropagation neural

network algorithm. Duan et al. [10] leveraged deep learning image recognition technology and the QT development platform, in conjunction with target damage tree analysis and Bayesian network inference methods, to provide a novel approach for predicting the damage effectiveness against large surface naval targets.

While these methods, predicated on neural networks and deep learning, demonstrate high predictive accuracy under conditions of Big Data, their performance often proves unsatisfactory when confronted with sparse datasets. Owing to the limited volume of data, such models are prone to overfitting the noise and local features within the training data, consequently leading to inadequate generalization capabilities on new, unseen data, and yielding predictions with considerable deviation. Furthermore, conventional data-driven models typically only learn the mapping relationships between inputs and outputs from the data, lacking an in-depth understanding and integration of physical laws. This deficiency allows models to generate results during the prediction process that may contravene fundamental physical principles, thereby diminishing the reliability and interpretability of the predictions and posing substantial risks in practical applications.

To address the limitations inherent in current methodologies, this paper innovatively proposes a Physics-Informed Neural Network (PINN) approach. This method quantifies the depth-velocity relationship of kinetic energy penetration [11-14], the overpressure attenuation law of blast shockwaves [15-17], the attenuation function of fragments perforating a target [18-20], and the critical angle conditions for ricochet [21-23] as physics-constrained objectives. It constructs a multi-mechanism coupled residual loss function, thereby constraining the neural network's training process with physical laws, and transforming the physical principles embedded within these models into mathematical constraints before integrating them into the neural network training regimen. By constructing a physics-based damage effectiveness model, the training of the neural network is constrained by the objective of minimizing the residual components of the physics-constrained model. This ensures that the neural network, while learning data features, simultaneously adheres to the constraints imposed by physical laws, thereby effectively enhancing predictive precision and achieving high-accuracy prediction of damage effectiveness under sparse data conditions.

This study presents several key contributions and innovations. Firstly, it deeply integrates an understanding of crucial physical processes, including penetration, explosion, fragmentation, and ricochet effects. Transcending conventional conceptual frameworks, it innovatively quantifies the complex physical damage process into parameters representing the potential contributions of different damage mechanisms. These parameters not only accurately reflect the extent of each mechanism's role throughout the entire damage process but also provide a robust foundation for establishing the physics-constrained objectives within the PINN framework. This enables the model to simulate the actual damage process with greater precision while rigorously maintaining physical consistency.

Secondly, the PINN method leverages prior physical knowledge to a significant extent, thereby effectively mitigating the model's reliance on large-scale datasets.

By integrating physical constraints into the neural network training, it addresses the overfitting and non-convergence issues frequently encountered in traditional learning models due to insufficient data. Under conditions of limited data availability, this approach still achieves high-precision predictions, markedly enhancing the model's stability and reliability. This offers a practical solution to damage effectiveness prediction in data-scarce operational environments.

Thirdly, this paper pioneers the application of PINN to the field of damage effectiveness, thereby opening a new research avenue in this domain. Through rigorous theoretical derivations and extensive experimental validation, the proposed method has been demonstrated to maintain a high degree of physical consistency in damage effectiveness prediction. The presented approach not only accurately predicts damage outcomes but also provides a physical-level explanation for the prediction process, enhancing the model's interpretability. Concurrently, across diverse experimental scenarios and data conditions, the method has consistently exhibited excellent effectiveness and robustness, offering a novel paradigm for modeling and predicting complex damage effects, and is poised to advance further developments in the field of munition damage effectiveness prediction.

2. Methodology

Addressing the challenges of predicting damage effectiveness for diverse targets in complex scenarios, particularly against the backdrop of sparse high-fidelity experimental or simulation data, traditional data-driven models often encounter issues of inadequate generalization capability and the possibility of prediction outcomes contravening physical laws. To surmount these limitations, this research proposes a Physics-Informed Neural Network (PINN) framework specifically for munition damage effectiveness prediction. The core tenet of this approach is the direct integration of established physical models, which describe key damage mechanisms, as physics constraints into the training process of a deep neural network, thereby leveraging physical knowledge to enhance the learning efficacy from sparse observational data.

2.1. Input Parameter Definition and Preprocessing

The performance of a Physics-Informed Neural Network (PINN) and the effective implementation of its physics constraints are highly contingent upon the precise definition and appropriate processing of the input vector x . The objective of this study is to construct a robust damage effectiveness prediction model, which takes as input a comprehensive input vector x encompassing munition characteristics, target attributes, and interaction parameters. This vector not only serves as the direct input to the neural network, driving its effectiveness prediction E^{PINN} , but also provides the requisite variables for the physics models to compute the physics-predicted effectiveness E_{phys} . Consequently, the input vector x must comprehensively encapsulate the critical factors influencing weapon damage effectiveness.

The input parameters selected in this study are designed to capture the core characteristics of the munition, the target, and their interaction, and they are

determined based on an understanding of key physical processes such as penetration, explosion, fragmentation, and ricochet. The specific parameter constitution, their physical significance, and their anticipated impact on damage effectiveness are detailed in Table 1:

Table 1 Parameter Constitution

Parameter Category	Parameter Name	Symbol	Physical Significance	Impact on Damage Effectiveness
Munition Attributes	Impact Velocity	v	Instantaneous velocity of the munition upon impacting the target.	Primarily determines kinetic energy and critical ricochet angle. Higher velocity generally results in greater penetration capability and higher effectiveness.
	Munition Mass	m	Overall mass of the munition.	Directly affects kinetic energy; greater mass leads to higher kinetic energy and typically higher penetration effectiveness.
	Equivalent Explosive Yield	y_{eq}	Energy released by munition detonation, expressed in TNT equivalent.	Determines blast shockwave intensity and initial fragment energy; larger yield results in higher explosion and fragment effectiveness.
	Munition Type	AT_1 AT_2	Boolean values: AT_1 indicates if the munition is a penetrator, AT_2 indicates if it is an explosive warhead.	Dictates the physical mechanisms considered by the model.
Target Attributes	Target Thickness	T	Material thickness of the main body of the target.	Increases penetration resistance and critical ricochet angle; greater thickness typically results in lower effectiveness.
	Target Material Strength	σ	Capacity of the material to resist deformation or fracture.	Increases resistance to penetration and blast/fragment damage. Higher strength generally results in lower effectiveness.
	Target Material Density	ρ	Mass per unit volume of the target material.	Influences fragment energy attenuation and critical ricochet angle. Density effects are complex, potentially increasing attenuation but also affecting ricochet behavior.
Interaction Parameters	Impact Angle	θ	Angle between the projectile trajectory and the normal to the target surface.	Critically affects ricochet and penetration/fragment path length. Larger angles increase ricochet probability and reduce effective penetration depth, typically lowering effectiveness.
	Standoff Distance	R	Distance from the detonation centre to the target evaluation point.	Determines blast shockwave intensity. Greater distance results in a weaker shockwave and lower blast effectiveness. Relevant only for explosive munitions.

To ensure the stability and efficiency of the neural network training, as well as to conform to its input requirements, preprocessing of the original parameters is necessary:

For continuous physical parameters, excluding munition type, either Z-Score Normalization or Min-Max Scaling is employed. Both methodologies map the data to comparable numerical ranges, thereby preventing certain features from exerting undue influence during gradient descent due to disparities in their magnitudes, while concurrently contributing to improved numerical stability. The parameters for standardization/normalization are computed based on the statistical properties of the training dataset.

The preprocessed parameter vector x' is subsequently fed into the input layer of the PINN. In the computation of the physics loss L_{phys} , the physics models utilize parameter values in their original physical units to ensure the correctness of the physical formulae.

2.2. Physics-Based Damage Effectiveness Model Construction

The cornerstone of the PINN methodology lies in embedding physical knowledge within the loss function of the neural network. For the problem of munition damage effectiveness prediction, it is necessary to construct mathematical models capable of characterizing the primary physical damage processes. We focus on four dominant mechanisms: kinetic energy penetration, blast shockwave loading, fragmentation effects, and ricochet phenomena. Considering the complexity or inapplicability of directly solving the governing partial differential equations (PDEs) [24-26], we opt for models widely accepted in engineering that can capture the core physical processes relevant to the final effectiveness.

Based on physical principles and empirical correlations, we construct the following physics-derived, dimensionless parameters aimed at quantifying the potential contribution of each primary damage mechanism:

Penetration Potential Π_p : Inspired by energy-based penetration models and based on the principle of energy conservation where the kinetic energy of the projectile is converted into plastic deformation energy of the target material, this parameter quantifies the ratio of projectile kinetic energy to target resistance. The normalized formula is:

$$\Pi_p = \frac{\frac{1}{2}mv^2}{\sigma \cdot T^2} \quad (1)$$

Explosion Potential Π_b : Originating from blast loading models, the peak overpressure ΔP_{phys} is first calculated based on the equivalent TNT yield y_{eq} and the standoff distance R . According to the Brode formula [28-29]:

$$\Delta P_{phys} = \frac{0.975 \cdot y_{eq}^{1/3}}{R} + \frac{1.455 \cdot y_{eq}^{2/3}}{R^2} + \frac{5.85 \cdot y_{eq}}{R^3} \quad (2)$$

Then, dimensionless processing of the peak overpressure using the target material strength:

$$\Pi_b = \frac{\Delta P_{phys}}{\sigma} \quad (3)$$

Fragmentation Potential Π_f : The initial kinetic energy of fragments E_{f0} attenuates exponentially as they pass through the target, due to material density ρ and penetration path length s . This parameter estimates the residual energy of fragments after perforating the target material and is normalized in the same manner as Π_p :

$$\Pi_f = \frac{E_{f0} \cdot e^{-k \cdot s \cdot \rho}}{\sigma \cdot T^2} \quad (4)$$

where k represents a material-dependent attenuation coefficient, E_{f0} can be calculated from the initial fragment velocity and mass, and s can be approximated based on target thickness T and impact angle θ .

These independent potential parameters are subsequently combined with weighting according to the munition type to form a comprehensive potential parameter, Π_c , reflecting the dominant damage mechanisms:

$$\Pi_c = (\omega_p \cdot \Pi_p) \cdot AT_1 + (\omega_b \cdot \Pi_b + \omega_f \cdot \Pi_f) \cdot AT_2 \quad (5)$$

where the weights $\omega_p, \omega_b, \omega_f$ serve to balance the dimensional scales and relative importance of different mechanisms and are adjustable or learnable model parameters.

This comprehensive potential is mapped to a basic physical effectiveness E_b via a saturation function, specifically:

$$E_b = 1 - e^{-\alpha \cdot \Pi_c} \quad (6)$$

where α is a scaling parameter controlling the saturation rate of effectiveness.

Finally, a ricochet effect correction is introduced. The critical ricochet angle θ_c is calculated based on impact conditions and material properties, with the specific formula being:

$$\theta_c = \arccos \left(\sqrt{\frac{\sigma \cdot T}{\rho \cdot v^2}} \right) \quad (7)$$

A smooth ricochet correction factor, f_r , is defined using a Sigmoid function centered around θ_c . When the actual impact angle θ (in radians) exceeds the critical angle, this factor sharply reduces the predicted effectiveness:

$$f_r = \sigma[-k_r \cdot (\theta - \theta_c)] = \frac{1}{1 + e^{k_r \cdot (\theta - \theta_c)}} \quad (8)$$

where k_r controls the steepness of the transition band.

The final physics-model-based predicted effectiveness E_f is obtained by multiplying the basic effectiveness by the ricochet correction factor:

$$E_f = f_r \cdot E_b \quad (9)$$

E_f is entirely derived from the integrated physical models and constitutes the physics-constrained target within the PINN framework.

2.3. Physics-Informed Neural Network Architecture and Training

The core computational engine of this research framework is a fully connected neural network, specifically a Multi-Layer Perceptron (MLP) [27], which is an advanced computational model used to identify complex functions via the backpropagation algorithm.

2.3.1. Network Architecture

The neural network receives the input vector x and outputs a scalar prediction of weapon damage effectiveness, E^{PINN} . The network employs a typical fully connected structure, comprising an input layer, multiple hidden layers, and an output layer.

In this study, the specific architecture of the PINN we constructed is as follows:

Input Layer: The number of neurons is equal to the dimensionality of the input vector x . As per Table 1, there are a total of 9 input neurons.

Hidden Layers: A total of 4 hidden layers are included.

Hidden Layer Neurons: Each hidden layer contains 128 neurons. The hidden layers utilize Tanh or Swish as the nonlinear activation function to enhance the network's expressive capability.

Output Layer: Contains 1 neuron, outputting the raw effectiveness prediction value. Since damage effectiveness E^{PINN} typically ranges between 0 and 1, the output layer employs a Sigmoid activation function to directly constrain the output within this interval, or alternatively, a linear activation function is used, with a Sigmoid transformation applied during the loss function calculation or for the final output.

The specific structure of the neural network is illustrated in Figure 1.

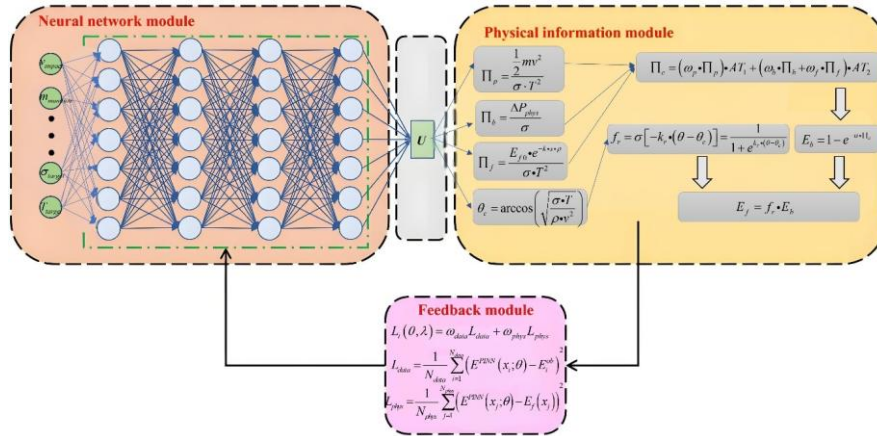


Fig. 1 The schematic diagram of PINN structure

2.3.2. Training Process

The training of the PINN is guided by a composite loss function, L_t , which linearly combines a data fidelity term and a physics-consistency term:

$$L_t(\theta, \lambda) = \omega_{data} L_{data} + \omega_{phys} L_{phys} \quad (10)$$

where θ represents the trainable weights and biases of the neural network, λ denotes parameters within the physics model that are designated as learnable during training (including $\omega_p, \omega_b, \omega_f$, etc.), and ω_{data} and ω_{phys} are weighting coefficients that balance the contributions of the two loss components.

The data loss, L_{data} , quantifies the discrepancy between the PINN predictions and the available observational data. It is typically formulated as the Mean Squared Error (MSE), computed over N_{data} observational data points x_i :

$$L_{data} = \frac{1}{N_{data}} \sum_{i=1}^{N_{data}} \left(E^{PINN}(x_i; \theta) - E_i^{ob} \right)^2 \quad (11)$$

where E_i^{ob} represents the experimentally measured damage effectiveness data corresponding to the observation point x_i .

The physics loss, L_{phys} , compels the network predictions to adhere to the comprehensive physical model constructed in Section 2.2. Unlike traditional PINNs that enforce zero residuals of PDEs, our approach constrains the neural network's prediction, E^{PINN} , to be consistent with the direct prediction from the physics model, E_f . This loss is evaluated on a set of N_{phys} collocation points x_j , which are sampled across the input parameter space, particularly in regions where observational data are scarce:

$$L_{phys} = \frac{1}{N_{phys}} \sum_{j=1}^{N_{phys}} \left(E^{PINN}(\cdot; \theta) - E_f(x_j; \lambda) \right)^2 \quad (12)$$

The network parameter θ , and potentially λ , are optimized by minimizing the total loss L_t using the gradient-based Adam optimization algorithm [30]. This process simultaneously drives the network to fit the sparse observational data and to adhere to the constraints imposed by the physics model over the input domain, as defined by the collocation points. The introduction of the physics loss acts as a potent regularization mechanism, contributing to an enhanced generalization capability of the model and ensuring the generation of physically plausible predictions even when training data are limited.

3. Results and Discussion

This chapter aims to systematically evaluate the performance of the proposed damage effectiveness prediction method, which is based on a PINN integrated with damage mechanisms, through a series of numerical experiments. Initially, high-fidelity finite element simulation data are acquired by simulating damage tests using the explicit dynamics module within the ANSYS simulation software. Subsequently, the predictive performance of the constructed PINN model is validated and benchmarked against a purely data-driven model devoid of physical information, with a particular focus on its performance under data-sparse conditions. Finally, the prediction results are presented via visualization techniques, and the advantages and implications of integrating physical information are discussed in depth.

3.1. Numerical Simulation Setup

The experimental data employed in this study were entirely derived from finite element simulations conducted using the ANSYS Explicit Dynamics module [31]. To emulate authentic damage experiments, simulations were performed in batches, distinguishing between two damage mechanisms: penetration and explosive fragmentation. The first batch constituted the dataset for penetration munitions, encompassing 30 distinct penetration processes and their resultant damage under varying parameters such as initial velocity, material hardness, and target plate thickness. The second batch comprised the dataset for blast munitions, simulating 30 scenarios of blast shockwave propagation and structural response under different equivalent yields, heights of burst (or contact points), and confinement conditions.

Taking penetration damage as an example, the projectile and target plate were created by inputting parameters such as mass, thickness, material density, and material strength. After mesh generation, simulation experiments were conducted by setting initial condition parameters, such as projectile initial velocity and flight angle, as well as boundary condition parameters, to generate corresponding damage contour plots. Figure 2 shows the damage effectiveness contour plot, depicting the extent of damage in different regions of the target; and the value of 1 signifies element failure.

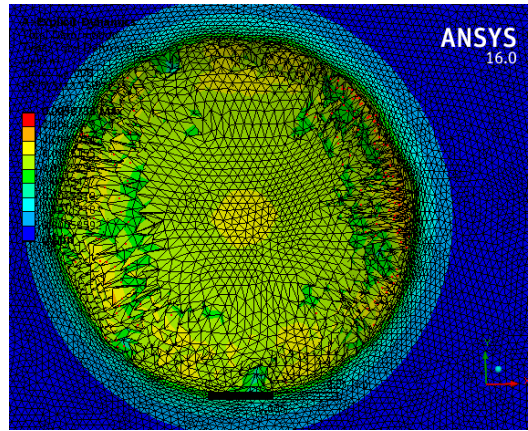


Fig. 2 Damage effectiveness diagram

3.2. Performance Comparison Analysis

The Physics-Informed Neural Network (PINN), by embedding relevant governing equations for damage effectiveness, can maintain high prediction accuracy even with sparse training data. This offers a novel approach to address the data dependency issue in munition effectiveness assessment in complex environments. To validate its advantages, this study conducts comparative experiments from multiple perspectives, benchmarking the PINN model against a purely data-driven Multilayer Perceptron (MLP), based on a small set of high-fidelity finite element simulation data from different scenarios.

3.2.1. Overall Prediction Accuracy

The most critical metrics for evaluating the performance of a model are its Root Mean Square Error (RMSE) and Mean Absolute Error (MAE) on the test dataset. These indicators intuitively reflect the accuracy with which each model predicts the target variable after being trained on the complete set of available training data. Following simulation, the experimental results are presented in Figures 3, 4, and 5.

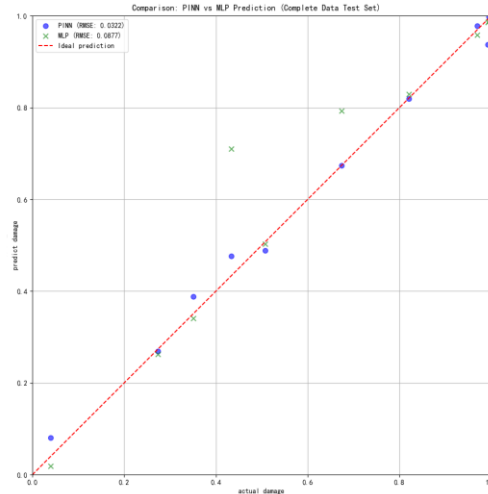


Fig. 3 Model prediction comparison chart

Figure 3 simultaneously displays, using different colors or marks, a comparison of the prediction points of both PINN and MLP against the true values on the test set. It is evident from the figure that the scatter points for PINN are more tightly clustered around the $y=x$ diagonal, with a lower RMSE value of 0.0322. In contrast, the scatter points for MLP are more disorganized, with some points significantly deviating from the $y=x$ diagonal, indicating that the MLP model systematically overestimates or underestimates the damage effectiveness values. Concurrently, its RMSE value of 0.0877 is also substantially higher than that of the PINN.

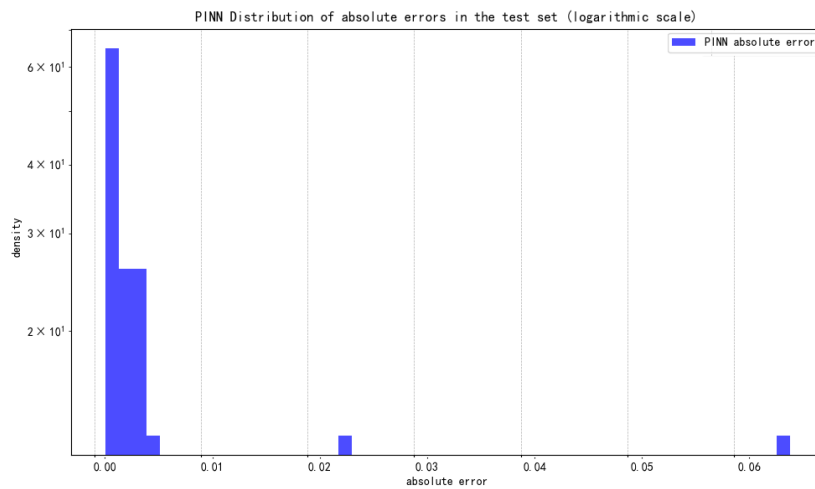


Fig. 4 Distribution chart of PINN absolute errors

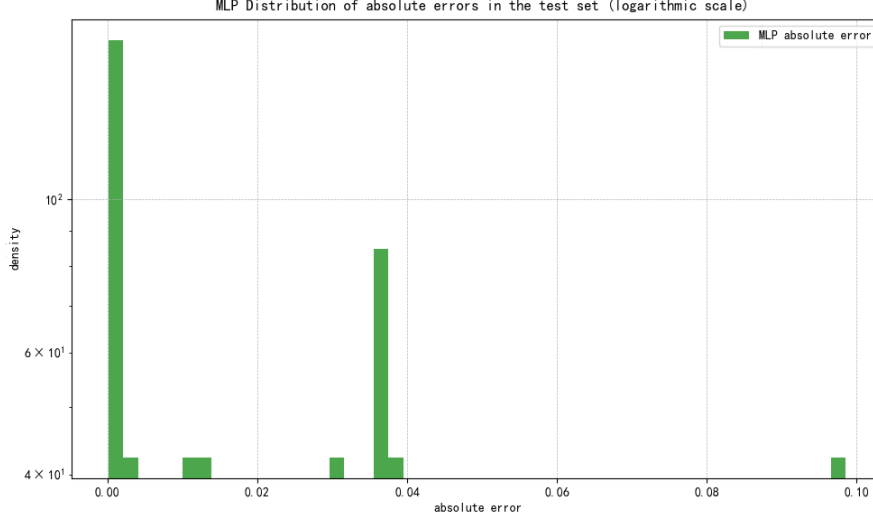


Fig. 5 Distribution chart of MLP absolute errors

Figures 4 and 5 respectively illustrate the absolute error distributions of PINN and MLP predictions on the test set after training with the complete dataset; to more intuitively represent the error distribution, the y-axis is set to a logarithmic scale. It can be observed from both figures that the error distributions are highly concentrated around 0, indicating that both models perform well, with most prediction errors being very small. However, compared to Figure 9, the tail of the distribution in Figure 8 is relatively more concentrated and shorter, signifying that PINN produces fewer large errors, rendering the model more stable.

Considering both RMSE and MAE for a comprehensive assessment, PINN, after being trained on the complete available training data, demonstrates superior performance in terms of prediction accuracy and stability.

3.2.2. Performance under Data-Sparse Conditions

In the contemporary armament domain, regarding the critical issue of munition damage effectiveness prediction, data acquisition frequently encounters numerous limitations, leading to a common prevalence of data sparsity. Consequently, comparing the performance of different models under data-sparse conditions assumes paramount importance.

This experiment investigates the sensitivity of model performance to the volume of training data by training both PINN and MLP models using subsets of 30%, 70%, and 100% of the training data, respectively. Specifically, it compares the performance of PINN and MLP under conditions of data sparsity by contrasting their RMSE values on the test set. To reduce training duration, the number of training epochs was changed from the previous 80,000 to 15,000 epochs per cycle. The specific results are illustrated in Figure 6.

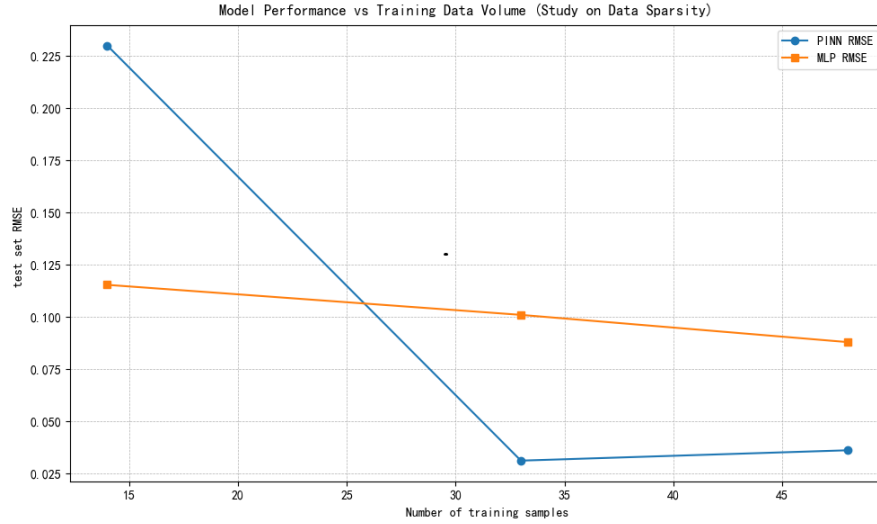


Fig. 6 Root Mean Square Error (RMSE) under different training data volumes

It can be observed from the figure that as the number of training samples increases, the RMSE for both PINN and MLP exhibits a downward trend, indicating that the models learn more information from a larger dataset. Although the RMSE curve for PINN is significantly higher than that of MLP when the data volume is small, its RMSE decreases more rapidly with an increase in data volume, reaching a lower plateau at 70% of the sample size. This suggests that PINN possesses better generalization capabilities under data-sparsity conditions and can make more effectively compensation by leveraging physical knowledge. As the sample size continues to increase, the marginal benefit diminishes substantially, indicating that PINN performs better with 70% of the sample data.

3.2.3. Physics Consistency Verification

Physics consistency is one of the key indicators for measuring whether a PINN has successfully integrated physical information into the model. A critical factor in quantifying physics consistency is the physical residual. Physics collocation points are points sampled within the domain where the physical equations are enforced, and they do not necessarily have corresponding labeled data. By substituting the model output into the physical equations at these points, residual values can be calculated. The physical residual represents the degree to which the model's prediction results adhere to the physical equations at the collocation points; the smaller the residual, the better the physics consistency. Following simulation, the experimental results are illustrated in Figures 7 and 8.

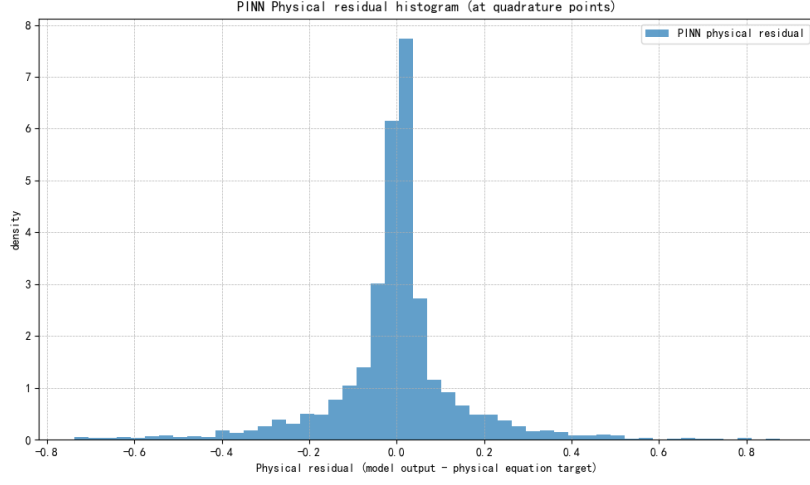


Fig. 7 PINN physical residual histogram

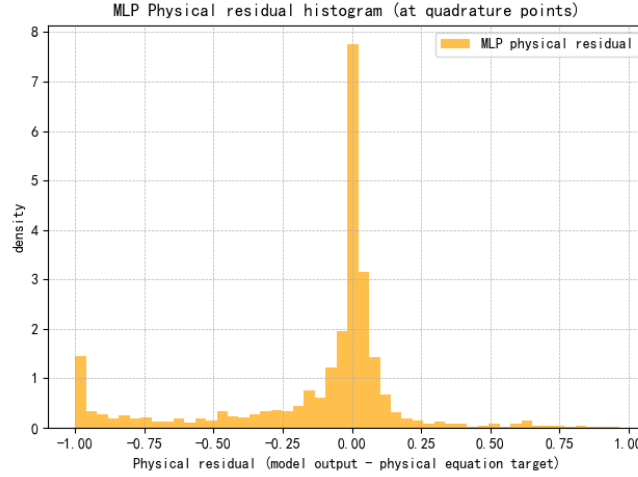


Fig. 8 MLP physical residual histogram

It is evident from Figure 7 that the histogram exhibits a relatively narrow distribution, a very light tail, and a peak extremely close to zero. This indicates that the physical residual values and their fluctuation range for PINN are very small at most collocation points, demonstrating good and consistent physical conformity.

In contrast, the physical residual distribution for MLP in Figure 8 is broader than that of PINN and possesses a longer tail, underscoring the limitations of purely data-driven methods in satisfying physical constraints. Concurrently, it intuitively demonstrates that PINN, through the introduction of physical constraints, achieves significant improvements in terms of physical consistency.

Considering the comprehensive experimental results, the trend exhibited by PINN aligns with the theoretical expectations regarding the influence of target thickness on damage effectiveness, demonstrating good physical consistency.

4. Conclusion

This research innovatively proposes a Physics-Informed Neural Network (PINN) model that achieves high-precision prediction of damage effectiveness in complex environments by organically integrating the physical mechanisms of munition damage with a deep learning framework. To comprehensively evaluate the performance of the PINN model, this study conducted systematic validations in multiple dimensions. Firstly, in terms of overall prediction performance, the PINN was benchmarked against a traditional Multilayer Perceptron (MLP) model. Experimental results demonstrated that on the same test dataset, the PINN achieved a 63.3% reduction in Root Mean Square Error (RMSE) and a 42.3% decrease in Mean Absolute Error (MAE), significantly enhancing prediction accuracy and stability. Secondly, to validate the model's performance under data-sparse conditions, comparative experiments were conducted using 30%, 70%, and 100% of the training data, respectively. The results showed that as the training data volume increased from 30% to 70%, the prediction error of the PINN rapidly decreased, fully substantiating its capability to effectively leverage physical knowledge to compensate for data insufficiency under sparse data conditions, thereby exhibiting excellent generalization ability. Furthermore, through comparisons of physics consistency verification, it was found that the PINN not only converged faster but also produced prediction results that strictly adhered to physical laws such as energy conservation, comprehensively confirming the model's high precision and robustness.

Despite the outstanding performance of the PINN model, limitations still exist under certain specific circumstances. When the impact velocity exceeded a threshold, thereby inducing an abrupt change in damage effectiveness, the PINN failed to completely reflect the true physical abrupt transition effect, leading to a reduction in prediction accuracy. This is primarily attributed to the inherent contradiction between the smoothing characteristics of neural networks and the phenomenon of physical abrupt changes. Addressing this issue, future improvement efforts should focus on refining the model. Enhancements such as introducing penalty terms for abrupt changes in the loss function and increasing the density of network nodes in regions of abrupt transitions could further elevate the model's predictive performance in complex physical scenarios, thereby providing more reliable technological support for munition damage effectiveness assessment.

Declaration of competing interest. The authors declare that they have no known competing interest to report regarding the present study.

References

- [1] Liu W, Duan Z, Liu Y, Numerical simulation of the damage and ignition responses of high explosives under low-velocity impact using the SPH method, *Engineering Analysis with Boundary Elements*, **166** (2024), 105830. <https://doi.org/10.1016/j.enganabound.2024.105830>

- [2] Wang K J, Rong G, Yi W J, Design and damage performance ability of supercavitation projectile with shaped charge, *Propellants, Explosives, Pyrotechnics*, **45** (4) (2020), 587-599. <https://doi.org/10.1002/prep.201900208>
- [3] He Z, Du Z, Zhang L, Damage mechanisms of full-scale ship under near-field underwater explosion, *Thin-Walled Structures*, **189** (2023), 110872. <https://doi.org/10.1016/j.tws.2023.110872>
- [4] Guo F, Xu W, Wei Y, Ignition mechanism and chemical reaction of the micro-damage polymer-bonded explosives under different inertial loading conditions, *Polymer Testing*, **137** (2024), 108532. <https://doi.org/10.1016/j.polymertesting.2024.108532>
- [5] Xue J, Li H, Zhang X, A damage effectiveness evaluation approach of warhead fragment group on missile target based on intuitionistic fuzzy neural network, *Journal of Mechanical Science and Technology*, **38** (9) (2024), 4765-4780. <https://doi.org/10.1007/s12206-024-0813-6>
- [6] Hou P, Pei Y, Ge Y, Adaptive fuze-warhead coordination method based on BP artificial neural network, *Defence Technology*, **29** (2023), 117-133. <https://doi.org/10.1016/j.dt.2022.12.006>
- [7] Wang L, Kong D, Study on correlation prediction model for static explosion and dynamic explosion shock wave pressure, *Measurement and Control*, **57** (7) (2024), 879-892. <https://doi.org/10.1177/00202940241227063>
- [8] Xu P, Shu J, Research on Damage Evaluation of Radar Target Based on Deep Learning, *IOP Conference Series: Materials Science and Engineering*. IOP Publishing, **569** (5) (2019), 052050. <https://doi.org/10.1088/1757-899x/569/5/052050>
- [9] Zhou K W, Ding S, Xie Y J, A neural network for the prediction of damage to reinforced cylindrical shells subjected to non-contact underwater explosions, *Journal of Physics: Conference Series*. IOP Publishing, **2891** (6) (2024), 062007. <https://doi.org/10.1088/1742-6596/2891/6/062007>
- [10] Duan C, Yin J, Wang Z, Design and Implementation of a Damage Assessment System for Large-Scale Surface Warships Based on Deep Learning, *Mathematical Problems in Engineering*, **1** (2022), 1462508. <https://doi.org/10.1155/2022/1462508>
- [11] Kim S, Kang T H K, Development of Energy-Based Impact Formula—Part I: Penetration Depth, *Applied Sciences*, **10** (14) (2020), 4964. <https://doi.org/10.3390/app10144964>

- [12] Basyir A, Agustian E S, Amelia A, A review of penetration tungsten-based projectile on depth of penetration at armor of ceramic-based, *Jurnal Pertahanan: Media Informasi tentang Kajian dan Strategi Pertahanan yang Mengedepankan Identity, Nasionalism dan Integrity*, **6** (3) (2020), 286-309. <https://doi.org/10.33172/jp.v6i3.890>
- [13] Basyir A, Bura R O, Lesmana D, Experimental consideration of projectile density and hardness effect on its penetration ability in alumina target, *Journal of Defense Acquisition and Technology*, **1** (1) (2019), 9-15. <https://doi.org/10.33530/jdaat.2019.1.1.9>
- [14] Young C W, Penetration equations, Sandia National Lab.(SNL-NM), Albuquerque, NM (United States), 1997.
- [15] Wu Z, Jin D, Yu B, Experimental and numerical investigation on shock wave attenuation in a chamber, *Scientific Reports*, **15** (1) (2025), 11468. <https://doi.org/10.1038/s41598-025-93836-2>
- [16] Wang L, Kong D, Xu C, Altitude influence on the explosion shock wave pressure distribution, *Journal of Measurements in Engineering*, **11** (3) (2023), 327-342. <https://doi.org/10.21595/jme.2023.23299>
- [17] Ye Z, Yang J, Yao C, Attenuation characteristics of shock waves in drilling and blasting based on viscoelastic wave theory, *International Journal of Rock Mechanics and Mining Sciences*, **171** (2023), 105573. <https://doi.org/10.1016/j.ijrmms.2023.105573>
- [18] Hong D, Li W, Zheng Y, Ballistic performance of spherical fragments penetrating PCrNi3MoV target plates, *Defence Technology*, **33** (2024), 295-307. <https://doi.org/10.1016/j.dt.2023.05.022>
- [19] Zhang X, Li H, A target damage assessment mathematical model and calculation method based on the intersection of warhead fragment and target mechanism, *Mathematics*, **10** (17) (2022), 3101. <https://doi.org/10.3390/math10173101>
- [20] Li H, Zhang X, Zhang X, Calculation model and method of target damage efficiency assessment based on warhead fragment dispersion, *IEEE Transactions on Instrumentation and Measurement*, **70** (2020), 1-8. <https://doi.org/10.1109/tim.2020.3017039>
- [21] Huang C L, Wang Z Q, Zhao S J, Critical ricochet angle of projectile penetrating into concrete, *Journal of Physics: Conference Series, IOP Publishing*, **2891** (5) (2024), 052012. <https://doi.org/10.1088/1742-6596/2891/5/052012>

- [22] Cho H, Choi M K, Park S, Determination of critical ricochet conditions for oblique impact of ogive-nosed projectiles on concrete targets using semi-empirical model, *International Journal of Impact Engineering*, **165** (2022), 104214. <https://doi.org/10.1016/j.ijimpeng.2022.104214>
- [23] Xue J, Shen P, Wang X, Research on ricochet and its regularity of projectiles obliquely penetrating into concrete target, *Journal of Vibroengineering*, **18** (5) (2016), 2754-2770. <https://doi.org/10.21595/jve.2016.16784>
- [24] Demo N, Strazzullo M, Rozza G, An extended physics informed neural network for preliminary analysis of parametric optimal control problems, *Computers & Mathematics with Applications*, **143** (2023), 383-396. <https://doi.org/10.1016/j.camwa.2023.05.004>
- [25] Mowlavi S, Nabi S, Optimal control of PDEs using physics-informed neural networks, *Journal of Computational Physics*, **473** (2023), 111731. <https://doi.org/10.1016/j.jcp.2022.111731>
- [26] Wang Y, Zhong L, NAS-PINN: Neural architecture search-guided physics-informed neural network for solving PDEs, *Journal of Computational Physics*, **496** (2024), 112603. <https://doi.org/10.1016/j.jcp.2023.112603>
- [27] Almeida L B, Multilayer perceptrons, *Handbook of Neural Computation*. CRC Press, (2020), C1. 2: 1-C1. 2: 30.
- [28] Song L, Yang Y, Zheng Z, Theoretical analysis and experimental study on physical explosion of stratospheric airship envelope, *Frontiers in Materials*, **9** (2023), 1046229. <https://doi.org/10.3389/fmats.2022.1046229>
- [29] Taha A K, Osman A, Zahran M S, Review of Blast Waves Analysis, Design, Structural and Materials Responses, *Open Journal of Safety Science and Technology*, **13** (2) (2023), 27-50. <https://doi.org/10.4236/ojsst.2023.132002>
- [30] Yang L, Theoretical Analysis of Adam Optimizer in the Presence of Gradient Skewness, *International Journal of Applied Science*, **7** (2) (2024), p27-p27. <https://doi.org/10.30560/ijas.v7n2p27>
- [31] Lee H H, Finite element simulations with ANSYS workbench 2023: Theory, applications, case studies, *SDC publications*, 2023.

Received: August 25, 2025; Published: September 10, 2025